

ing and embossing individual layers of NC–titania composites and then planarizing the structure with a neat film of titania.

Optical Characterization: Optical excitation with a frequency-doubled, regeneratively amplified titanium-sapphire laser (3.1 eV photons, 1 kHz repetition rate, 100 fs pulse width) was used to characterize the output characteristics of these functional nanodevices. The average pump power was adjusted using calibrated neutral density filters. The laser beam was focused using a cylindrical lens. The light emitted approximately normal to the heterostructure was detected with a fiber optic assembly in the far-field (detection angle $\approx 2^\circ$) coupled to a grating spectrometer that used a charge-coupled device (CCD) camera as the time-integrating detection device.

AFM Characterization: The samples were imaged using an atomic force microscope (Digital Instruments, Nanoscope III) in tapping mode.

Received: January 11, 2004
Final version: May 19, 2004

Surface-Initiated Polymerization on Nanopatterns Fabricated by Electron-Beam Lithography**

By Sang Jung Ahn, Marian Kaholek, Woo-Kyung Lee, Bruce LaMattina, Thomas H. LaBean, and Stefan Zauscher*

Surface-initiated polymerization (SIP) of polymer brushes^[1] can be used to tailor the surface properties of materials by imparting desirable chemical, surface-energetic, mechanical, and electrical functionalities.^[2,3] Exerting control over polymer functionality, shape, feature dimension, and inter-feature spacing on the nanometer length scale is attractive because nanopatterned polymer-brush structures can be exploited in sensors,^[4] combinatorial arrays,^[5] protein-affinity separations,^[6] and in micro- and nanofluidic devices.^[7] Several studies demonstrated the fabrication of patterned polymeric structures in a “grafting-from” approach using microcontact printing,^[8–13] photolithography,^[14] chemical lithography,^[15] electron-beam lithography (EBL),^[16] contact molding,^[17] scanning probe lithography (SPL),^[18–21] and two-photon photopolymerization.^[22] Although significant progress has been made in the templated fabrication of polymer brushes,^[23] preparation of precisely patterned, surface-attached polymeric micro- and nanostructures with controlled chain lengths, chemical functionalities, shapes, feature dimensions, and inter-feature spacings is still in the developmental stage.

Herein we report a new “top-down/bottom-up” approach for fabricating patterned polymer-brush arrays on the micrometer and nanometer length scales. In our approach, a silicon surface is patterned with gold (Au) using lift-off (dissolution) electron-beam lithography (“top-down”).^[24] The resulting pattern is then amplified by surface-initiated polymerization (“bottom-up”) from an immobilized thiol initiator^[25] using atom transfer radical polymerization (ATRP).^[26] Our approach has several advantages over existing polymer nanopatterning methods. First, patterns with well-defined feature di-

- [1] R. Phelan, V. Weldon, M. Lynch, J. F. Donegan, *Electron. Lett.* **2002**, *38*, 31.
- [2] J. Faist, F. Capasso, C. Sirtori, D. L. Sivco, A. L. Hutchinson, A. Y. Cho, *Nature* **1997**, *387*, 777.
- [3] B. Zhao, A. Yariv, in *Semiconductor Lasers I: Fundamentals* (Ed.: E. Kapon), Academic Press, San Diego, CA **1999**.
- [4] Y. Arakawa, H. Sakaki, *Appl. Phys. Lett.* **1982**, *40*, 939.
- [5] M. Asada, Y. Miyamoto, Y. Suematsu, *IEEE J. Quantum Electron.* **1986**, *22*, 1915.
- [6] C. B. Murray, C. R. Kagan, M. G. Bawendi, *Annu. Rev. Mater. Sci.* **2000**, *30*, 545.
- [7] V. I. Klimov, A. A. Mikhailovsky, S. Xu, A. V. Malko, J. A. Hollingsworth, C. A. Leatherdale, H.-J. Eisler, M. G. Bawendi, *Science* **2000**, *290*, 314.
- [8] V. C. Sundar, H.-J. Eisler, M. G. Bawendi, *Adv. Mater.* **2002**, *14*, 739.
- [9] M. A. Petruska, A. V. Malko, P. M. Voyles, V. I. Klimov, *Adv. Mater.* **2003**, *15*, 610.
- [10] M. Kazes, D. Y. Lewis, Y. Ebenstein, T. Mokari, U. Banin, *Adv. Mater.* **2002**, *14*, 317.
- [11] H.-J. Eisler, V. C. Sundar, M. G. Bawendi, M. Walsh, H. I. Smith, V. I. Klimov, *Appl. Phys. Lett.* **2002**, *80*, 4614.
- [12] T. Hidaka, Y. Hatano, *Electron. Lett.* **1991**, *27*, 1075.
- [13] M. C. Farries, A. C. Carter, G. G. Jones, I. Bennion, *Electron. Lett.* **1991**, *27*, 1498.
- [14] Y. Xia, G. M. Whitesides, *Angew. Chem. Int. Ed.* **1998**, *37*, 551.
- [15] H. Kogelnik, C. V. Shank, *Appl. Phys. Lett.* **1971**, *18*, 152.
- [16] H.-J. Eisler, V. C. Sundar, M. G. Bawendi, *Appl. Phys. Lett.*, in press.
- [17] S. Y. Chou, P. R. Krauss, P. J. Renstrom, *J. Vac. Sci. Technol., B* **1996**, *14*, 4129.

[*] Prof. S. Zauscher, Dr. M. Kaholek, W.-K. Lee
Department of Mechanical Engineering and Materials Science and
Center for Biologically Inspired Materials and Material Systems
Duke University
Durham, NC 27708 (USA)
E-mail: zauscher@duke.edu
Dr. S. J. Ahn, Prof. T. H. LaBean
Department of Computer Science, Duke University
Durham, NC 27708 (USA)
Dr. B. LaMattina
Army Research Office
PO Box 12211, Research Triangle Park, NC 27709 (USA)

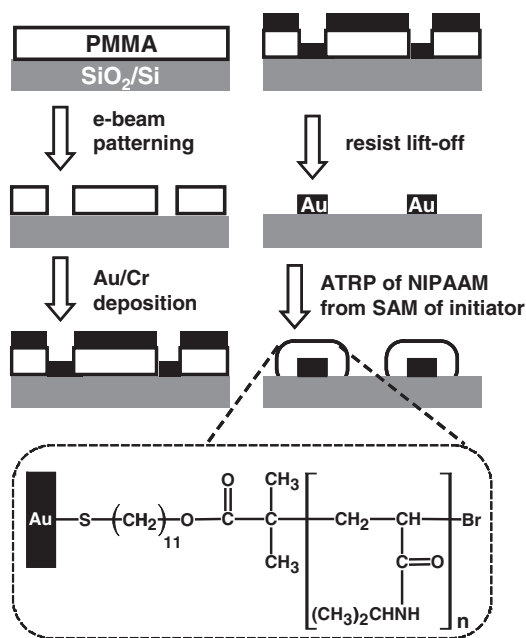
[**] Sang Jung Ahn and Marian Kaholek contributed equally to this work. The authors thank the National Science Foundation for support through grants NSF EEC-021059, NSF DMR-0239769 CAREER AWARD, and ARO DAADG55-98-D-0002. We thank Mr. Hongwei Ma (Department of Biomedical Engineering, Duke University) for the synthesis of the thiol initiator.

mensions, shapes, and inter-feature spacings can be easily created over large areas by lift-off EBL. Second, Au-patterned silicon substrates facilitate the fabrication of mixed-polymer brushes^[27] with high lateral resolution by using silane- and thiol-containing initiators immobilized onto silicon and gold surfaces, respectively. Third, the combination of lift-off EBL and ATRP allows the fabrication of covalently attached, high-density polymer-brush arrays with a wide choice of monomers and chemical functionalities. To explore the potential of our approach, we demonstrate surface-initiated polymerization of stimulus-responsive polymer brushes on Au-patterned silicon surfaces.

To test the polymerization chemistry, we first immobilized the thiol initiator ω -mercaptoundecyl bromoisobutyrate ($\text{BrC}(\text{CH}_3)_2\text{COO}(\text{CH}_2)_{11}\text{SH}$)^[25] and then polymerized *N*-isopropylacrylamide (NIPAAm) on unpatterned, Au-coated silicon substrates using ATRP.^[28] The polymerization reaction was carried out at room temperature by exposing the initiator-decorated substrates for 60 min to the reaction medium, which contained NIPAAm in water with a low methanol (MeOH) concentration (2.6 vol.-%). This MeOH concentration does not affect the lower critical solution temperature (LCST) behavior of poly(*N*-isopropylacrylamide) (pNIPAAm), and the growing polymer brush thus adopts an extended conformation.^[29,30] In ATRP, a highly reactive, and in our case surface-tethered, organic radical is generated along with a stable Cu(II) species that can be regarded as a persistent metalloradical that is not able to initiate radical polymerization in the polymerizing solution.^[26] Consequently, the polymerization reaction is strictly confined to the surface-attached growing polymer chains. Analysis of the substrate surface with reflectance Fourier-transform IR (FTIR) spectroscopy, atomic force microscopy (AFM), and ellipsometry revealed that after a 60 min polymerization time, the surfaces were homogeneously covered by a 250 nm thick pNIPAAm-brush layer.^[31]

Scheme 1 illustrates our patterning and polymerization approach. We first used lift-off EBL to pattern a silicon substrate.^[24] We then created a self-assembled monolayer (SAM) of thiol initiator on the Au-patterns to initiate brush growth there, and finally we amplified the initiator pattern by ATRP of NIPAAm.

Tapping mode AFM height images ($80\ \mu\text{m} \times 80\ \mu\text{m}$) in air and corresponding averaged-height profiles for Au lines fabricated by the lift-off procedure on a silicon substrate and the resulting pNIPAAm-brush line micropattern are shown in Figures 1a,b, respectively. The Au lines in Figure 1a all have typical dimensions (measured by AFM) of $1.5\ \mu\text{m} \times 50\ \mu\text{m} \times 40\ \text{nm}$ (width \times length \times height), but vary in their relative spacing, ranging from 0.5–6 μm . Figure 1b shows the pNIPAAm-brush lines prepared by ATRP on the patterned substrate, using the same polymerization conditions as for the bulk brushes, with the exception of the polymerization time, which was 90 min. Figure 1b shows that brush growth is uniform and that brush height is not affected by line spacing. The dry pNIPAAm-brush lines have a height of about 300 nm (after subtraction of 40 nm for the Au–Cr layer) and a width



Scheme 1. Preparation of surface-confined pNIPAAm polymer-brush patterns by combining lift-off electron-beam lithography (EBL) and surface-initiated ATRP using a surface-tethered thiol initiator.

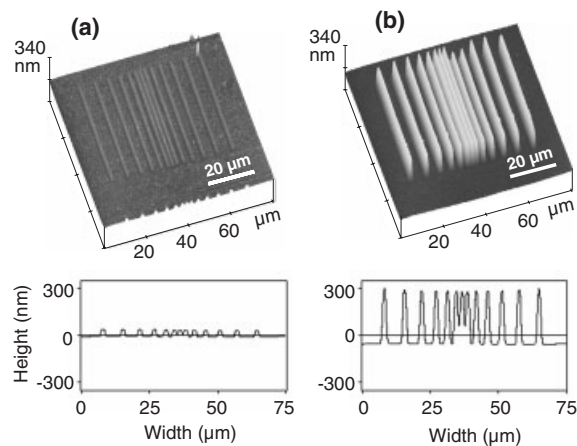


Figure 1. Tapping-mode AFM height images obtained at room temperature in air and the corresponding average-height profiles. a) Au-line pattern (1.5 μm wide, 40 nm high) fabricated by lift-off EBL. b) pNIPAAm-brush line pattern (1.8 μm wide, 300 nm high) after 90 min polymerization time, prepared using surface-initiated ATRP from immobilized thiol initiator on the Au-line pattern.

of about 1.8 μm , measured with AFM at a height of about 170 nm. The polymer-brush lines are wider than the underlying gold patterns. This is expected, considering that polymer growth also occurs laterally on the 40 nm high gold templates (see below).

When we reduced the lateral dimensions of the Au features to $250\ \text{nm} \times 250\ \text{nm}$ square dots, we observed that the polymer-brush height on these nanopatterns was significantly less than that on the $1.5\ \mu\text{m} \times 50\ \mu\text{m}$ line patterns under otherwise

identical polymerization conditions. To study this effect more closely, we patterned a substrate with both micro- and nano-scale features and amplified the pattern by surface-initiated ATRP of NIPAAM. An AFM tapping-mode image of the resulting pNIPAAM-brush pattern is shown together with a typical cross-section in Figure 2. Figure 2 shows that there is a significant difference in dry-brush height between the micro-scale line patterns (brush height of about 300 nm) and nano-scale dot patterns (brush height of about 170 nm).

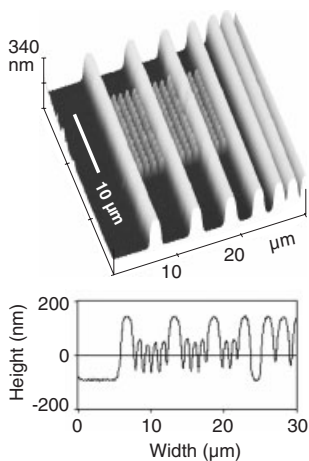


Figure 2. Tapping-mode AFM height image obtained at room temperature in air and corresponding average-height profile of a combined pNIPAAM-brush line micropattern (1.8 μm wide, 300 nm high) and a dot nanopattern (600 nm wide, 170 nm high), fabricated using lift-off EBL and surface-initiated ATRP after 90 min polymerization time.

We believe that this behavior can be explained by considering the effective initiator surface density and chain crowding. The polymer-brush conformation results from a balance between segment interactions and elastic free energies. While dense tethering enforces strong overlapping of the segments of undeformed coils and increases the interaction energy, chain stretching lowers this interaction energy at the price of increased elastic free energy. We assume a uniform initiator density that is independent of pattern size; i.e., initiator self-assembly is not affected by the lateral dimensions of the gold pattern. This is reasonable because our smallest lateral feature dimension is still two orders of magnitude larger than the molecular size of the initiator thiol. Furthermore, we assume that the initiator efficiency is independent of pattern size. Both assumptions are supported by our observation that lateral polymer-brush growth with brush heights similar to those on top of the Au nanopatterns also occurs on the sides of these 40 nm high patterns (see Fig. 3, below). A polymer brush likely adopts a vertically less-ordered and laterally more-extended conformation when the brush height approaches the lateral-feature dimensions (dictated here by the lateral size of the underlying Au pattern). This disorder can be understood by the lack of restraint the brush experiences at its boundaries, leading to less chain crowding and thus less chain

stretching. Together with the potentially small number of effectively initiated chains on small patterns—there are simply fewer polymer-chain neighbors due to the proximity of the pattern boundaries—this can, at least qualitatively, explain our observations. An in-depth study of the dependence of brush height on pattern size is currently underway in our laboratory.

Scanning electron microscopy (SEM) images (Fig. 3) show that lateral polymer-brush growth also occurs on the sides of

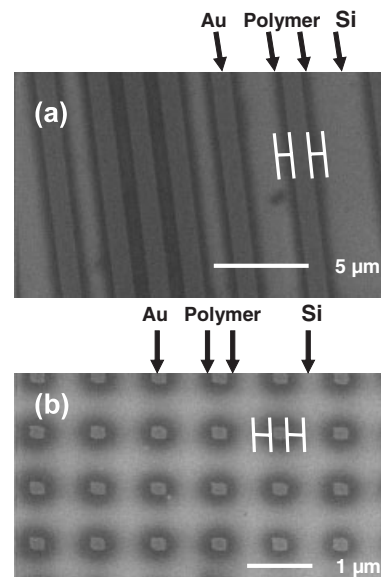


Figure 3. Scanning electron microscopy (SEM) image of a) pNIPAAM-brush line pattern and b) dot pattern after 90 min polymerization time. The micrograph shows the boundaries between the polymer brush (dark regions), the initial Au features (light regions) and the silicon surface (light regions). The darker lines in Figure 3a represent an approximately 530 nm wide brush grown laterally on the 1.15 μm wide Au lines (light). The darker corona in Figure 3b represents an approximately 220 nm wide brush grown laterally on the 210 nm wide Au squares (light). The white lines (H-shapes) schematically illustrate the polymer-brush growth on the sides of the 40 nm high gold templates.

the 40 nm high Au patterns. Polymer appears as approximately 530 nm wide dark lines flanking the 1.15 μm wide brighter Au lines in Figure 3a, and the darkened coronas (about 220 nm wide) around the 210 nm wide brighter Au squares in Figure 3b. These SEM images reveal that the lateral polymer-feature size is similar to the brush height on the top of patterns as measured by tapping-mode AFM. When using our patterning approach, lateral brush growth needs to be considered, as it can potentially compromise the lateral feature resolution of nanopatterned polymer brushes and can interfere in the fabrication of laterally separated, distinct polymer brushes using a dual-initiation scheme.

The effect of solvent conditions^[29,30] on the conformation of patterned (13 dots \times 13 dots), stimulus-responsive pNIPAAM brushes is demonstrated in Figure 4. When the dry pNIPAAM brush pattern is exposed to pure water at a temperature below

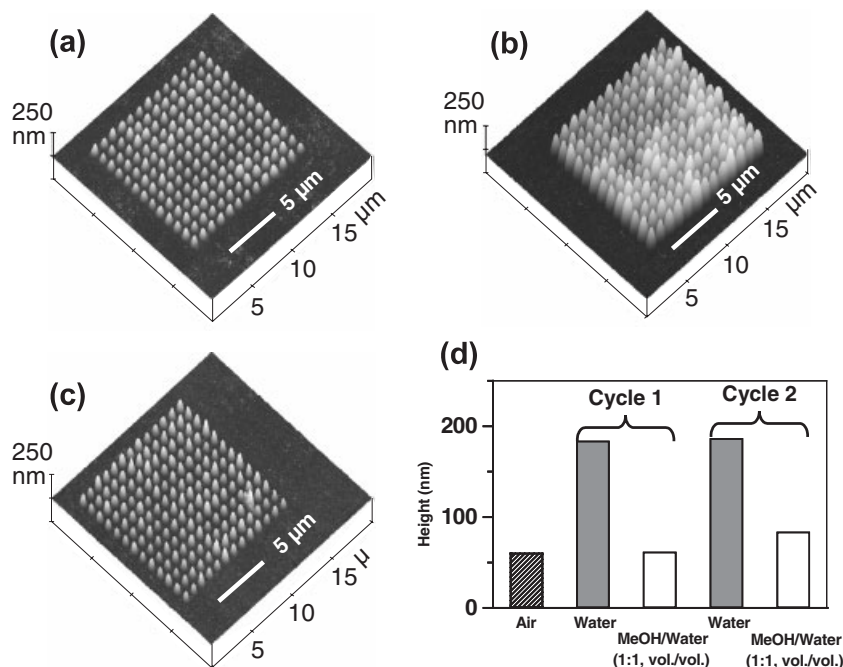


Figure 4. pNIPAAAM-brush dot array (90 min polymerization time) imaged at room temperature in a) air, b) Milli-Q (MQ)-grade water, and c) a mixture of MeOH/water (1:1, vol./vol.) using contact-mode AFM. d) Average brush height plotted as a function of solvent condition in air (patterned bar; brush collapsed) and after cyclic exposure (two cycles), first to MQ-grade water (gray bars; brush swollen), and then to a 1:1 (vol./vol.) MeOH/water mixture (white bar; brush collapsed).

the LCST (a good solvent), the polymer brush swells significantly and triples its height (Figs. 4a,b,d). After exposure to a water-methanol (1:1, vol./vol.) mixture (a poor solvent), the brush adopts a hydrophobically collapsed conformation (Figs. 4c,d).^[21] Cyclic exposure to water and a water-methanol mixture (1:1, vol./vol.) showed that this solvent-induced phase transition is reversible (Fig. 4d).

In summary, we have demonstrated the utility of combining lift-off EBL for fabrication of Au patterns and surface-initiated polymerization to form micro- and nanostructures of stimulus-responsive (“smart”) polymer brushes on silicon surfaces. Nanopatterned polymer brushes with inducible phase-transition behavior, such as pNIPAAAM, can likely be exploited for protein-affinity separations^[6] and as switches in nano- and microfluidic devices.^[7]

Our fabrication approach allows a high level of lateral control in patterning surfaces with complex polymer-brush structures over large surface areas. Due to the “living” character of ATRP initiators, we believe that patterned copolymer brushes can also be fabricated.^[26] Although the minimum attainable dimension of patterned features has not yet been explored, we expect that further improvements in the EBL process, such as the use of SAM resists^[32] or two-layer electron-sensitive resists,^[24] in order to minimize both the forward scattering of electrons through the sensitive resist layer, and the backscattering of electrons from the substrate, will result in considerably reduced feature dimensions.

Experimental

Lift-off Electron-Beam Lithography: A 130 nm thick one-layer electron-sensitive resist film of poly(methyl methacrylate) (PMMA, weight-average molecular weight $M_w = 950\,000\text{ g mol}^{-1}$) was spin-coated onto a previously cleaned Si substrate and annealed at 160 °C on a hot plate for 20 min. The resist layer was then patterned by exposure to an electron beam, using a Philips FEI XL30 Thermal Field Emitter scanning electron microscope (SEM) (operating current 144 pA, accelerating voltage 30 kV, working distance 7.5 mm, electron-beam spot size 3 nm, chamber pressure 1.0×10^{-3} Pa) controlled by Nano Pattern Generator System (NPGS) software. The exposed PMMA layer was developed in a solution of methyl isobutyl ketone (MIBK) and isopropyl alcohol (IPA) (1:3 vol./vol.) for 80 s, quenched by IPA for 20 s, and finally isolated by rinsing with deionized water. A layer of chromium (50 Å) and a layer of gold (350 Å) were thermally evaporated onto the patterned PMMA/silicon substrate under vacuum (2×10^{-4} Pa) at room temperature to obtain geometrically well-defined gold features on the exposed SiO₂ surface. The Au-coated, developed resist was lifted-off (dissolved) by immersing the substrate in boiling acetone (60 °C), leaving behind 40 nm thick Au patterns on the silicon substrate. The patterned silicon substrate was finally rinsed with copious amounts of acetone and blown dry in a stream of N₂.

Initiator Monolayers: The atom transfer radical polymerization (ATRP) initiator, ω-mercaptopundecyl bromoisobutyrate (BrC(CH₃)₂COO-(CH₂)₁₁SH), was synthesized as reported [25]. A self-assembled monolayer (SAM) of the bromo initiator on the gold patterns was obtained by immersing the substrate in a 1 mM ethanolic solution of the thiol initiator for 48 h.

N-isopropylacrylamide (NIPAAAM) Polymerization: We used ATRP to prepare surface-attached poly(N-isopropylacrylamide) brushes of controlled structure [21,33,34]. Prior to use, all solutions and flasks were thoroughly flushed with dry nitrogen gas to remove oxygen. The polymerization solution (similar for the bulk and patterned brushes) was prepared by adding a solution of NIPAAAM monomer to an organometallic catalyst. The organometallic catalyst was formed in a nitrogen atmosphere by adding Cu(I)Br (2.5 mg, 0.017 mmol) and N,N,N',N',N''-pentamethyldiethyltri-amine (PMDETA, 18 μL, 0.086 mmol) in a 1:5 molar ratio to 1 mL of MeOH as solvent. The mixture was then sonicated for 1–2 min to facilitate the formation of the Cu^IBr/PMDETA complex. Next, 8.4 g (74 mmol) of NIPAAAM monomer dissolved in 38 mL of water (18 wt.-%) was filtered into the catalyst-complex solution through a 0.45 μm Millipore Millex filter. The molar ratio of NIPAAAM to Cu^I was fixed at 4300:1 at a volume ratio of MeOH to water of 1:38 for all polymerizations. The polymerization solution was then transferred into flasks containing the initiator-functionalized substrates. The bulk and patterned pNIPAAAM brushes were synthesized by polymerization for 60 min and 90 min, respectively, without stirring at room temperature under nitrogen. Substrates were then removed from the polymerization solution and immediately rinsed with copious amounts of Milli-Q water to remove all traces of the polymerization solution, and subsequently dried under a stream of nitrogen. As a check for the presence of polymer in solution, an aqueous polymerizing solution was poured into an equal volume of MeOH at room temperature to induce a phase transition. The absence of precipitation of polymer in the solution indicated that no polymerization took place in solution.

Characterization: Reflectance Fourier-transform spectra were recorded on a Thermo Nicolet Nexus 670 spectrometer. Ellipsometric measurements of dried brushes were obtained with a custom-built null-ellipsometer with a He–Ne laser (632.8 nm) light source and a 70.0° angle of incidence. Atomic force microscopy (AFM) images were obtained by contact mode and tapping mode imaging using V-shaped silicon nitride cantilevers (NanoProbe, Veeco, Santa Barbara, CA; spring constant 0.12 N m⁻¹, tip radius 20–60 nm) using a MultiMode scanning probe microscope (SPM) and a Dimension 3100 SPM (Veeco, Santa Barbara, CA). Topographic imaging was performed in air, in water, and in water–MeOH (1:1, vol./vol.) mixtures using a fluid cell. Image forces were kept below 1 nN to minimize compression and damage to polymer brushes. All SEM images were taken at 30 kV (accelerating voltage) in the same SEM used in electron-beam lithography.

Received: July 3, 2004

Final version: September 18, 2004

- [1] O. Prucker, J. Rühle, *Macromolecules* **1998**, *31*, 592.
- [2] B. Zhao, W. J. Brittain, *Prog. Polym. Sci.* **2000**, *25*, 677.
- [3] *Polymer Brushes: Synthesis, Characterization, Applications* (Eds: R. C. Advincula, W. J. Brittain, K. C. Caster, J. Rühle), Wiley-VCH, Weinheim, Germany **2004**.
- [4] R. C. Bailey, J. T. Hupp, *Anal. Chem.* **2003**, *75*, 2392.
- [5] M. P. Stoykovich, H. B. Cao, K. Yoshimoto, L. E. Ocola, P. F. Nealey, *Adv. Mater.* **2003**, *15*, 1180.
- [6] N. Nath, A. Chilkoti, *Adv. Mater.* **2002**, *14*, 1243.
- [7] D. J. Beebe, J. S. Moore, Q. Yu, R. H. Liu, M. L. Kraft, B. H. Jo, C. Devadoss, *Proc. Natl. Acad. Sci. U. S. A.* **2000**, *97*, 13 488.
- [8] Y. N. Xia, G. M. Whitesides, *Angew. Chem. Int. Ed.* **1998**, *37*, 551.
- [9] N. L. Jeon, I. S. Choi, G. M. Whitesides, N. Y. Kim, P. E. Laibinis, Y. Harada, K. R. Finnie, G. S. Girolami, R. G. Nuzzo, *Appl. Phys. Lett.* **1999**, *75*, 4201.
- [10] M. Husemann, D. Mecerreyes, C. J. Hawker, J. L. Hedrick, R. Shah, N. L. Abbott, *Angew. Chem. Int. Ed.* **1999**, *38*, 647.
- [11] D. M. Jones, W. T. S. Huck, *Adv. Mater.* **2001**, *13*, 1256.
- [12] W. F. Guo, G. K. Jennings, *Adv. Mater.* **2003**, *15*, 588.
- [13] J. Hyun, A. Chilkoti, *Macromolecules* **2001**, *34*, 5644.
- [14] O. Prucker, M. Schimmel, G. Tovar, W. Knoll, J. Rühle, *Adv. Mater.* **1998**, *10*, 1073.
- [15] U. Schmelmer, R. Jordan, W. Geyer, W. Eck, A. Golzhauser, M. Grunze, A. Ulman, *Angew. Chem. Int. Ed.* **2003**, *42*, 559.
- [16] Y. Tsujii, M. Ejaz, S. Yamamoto, T. Fukuda, K. Shiget, K. Mibu, T. Shinjo, *Polymer* **2002**, *43*, 3837.
- [17] T. A. von Werne, D. S. Germack, E. C. Hagberg, V. V. Sheares, C. J. Hawker, K. R. Carter, *J. Am. Chem. Soc.* **2003**, *125*, 3831.
- [18] X. G. Liu, S. W. Guo, C. A. Mirkin, *Angew. Chem. Int. Ed.* **2003**, *42*, 4785.
- [19] B. W. Maynor, S. F. Filocamo, M. W. Grinstaff, J. Liu, *J. Am. Chem. Soc.* **2002**, *124*, 522.
- [20] Y. Okawa, M. Aono, *Nature* **2001**, *409*, 683.
- [21] M. Kaholek, W.-K. Lee, B. LaMattina, K. C. Caster, S. Zauscher, *Nano Lett.* **2004**, *4*, 373.
- [22] P. J. Campagnola, D. M. Delguidice, G. A. Epling, K. D. Hoffacker, A. R. Howell, J. D. Pitts, S. L. Goodman, *Macromolecules* **2000**, *33*, 1511.
- [23] D. J. Dyer, *Adv. Funct. Mater.* **2003**, *13*, 667.
- [24] R. E. Howard, E. L. Hu, L. D. Jackel, P. Grabbe, D. M. Tennant, *Appl. Phys. Lett.* **1980**, *36*, 592.
- [25] D. M. Jones, A. A. Brown, W. T. S. Huck, *Langmuir* **2002**, *18*, 1265.
- [26] K. Matyjaszewski, J. H. Xia, *Chem. Rev.* **2001**, *101*, 2921.
- [27] L. Ionov, S. Minko, M. Stamm, J.-F. Gohy, R. Jerome, A. Scholl, *J. Am. Chem. Soc.* **2003**, *125*, 8302.
- [28] M. Kaholek, W.-K. Lee, S. J. Ahn, H. Ma, K. C. Caster, B. LaMattina, S. Zauscher, *Chem. Mater.* **2004**, *16*, 3688.
- [29] F. M. Winnik, H. Ringsdorf, J. Venzmer, *Macromolecules* **1990**, *23*, 2415.
- [30] H. G. Schild, M. Muthukumar, D. A. Tirrell, *Macromolecules* **1991**, *24*, 948.
- [31] The reflectance FTIR spectra of the rinsed surfaces confirmed that a layer of covalently attached pNIPAAm was formed. Typical absorption bands [cm⁻¹]: secondary amide –NH stretching, 3301; asymmetric stretching of the –CH₃ group, 2970; asymmetric stretching of the –CH₂– group, 2932; symmetric stretching of the –CH₃ group, 2874; secondary amide C=O stretching, 1645; secondary amide –NH stretching, 1538; asymmetric bending deformation of –CH₃ group, 1458; and the deformation of the two –CH₃ groups on the isopropyl functionality, 1386 and 1366.
- [32] A. Golzhauser, W. Geyer, V. Stadler, W. Eck, M. Grunze, K. Edinger, T. Weimann, P. Hinze, *J. Vac. Sci. Technol., B: Microelectron. Nanometer Struct.—Process., Meas., Phenom.* **2000**, *18*, 3414.
- [33] D. M. Jones, J. R. Smith, W. T. S. Huck, C. Alexander, *Adv. Mater.* **2002**, *14*, 1130.
- [34] S. Balamurugan, S. Mendez, S. S. Balamurugan, M. J. O'Brien, G. P. Lopez, *Langmuir* **2003**, *19*, 2545.

Discontinuous Molecular Films Can Control Metal/Semiconductor Junctions**

By Hossam Haick, Marianna Ambrico, Teresa Ligonzo, and David Cahen*

The use of molecules in (opto)electronic devices is attractive because of the variety and flexibility of their functions.^[1,2,3] In this respect, hybrid devices, in which molecular functionality serves to influence and control the characteristics of “classical” electronic devices, have a potential advantage over other approaches to molecular electronics, in that they impose far fewer limitations on the choice of molecules that can be used.^[4] This is so because, as we shall show here, the molecules can function as gatekeepers, rather than providing the sole path for current transport between electrodes. Added advantages could be increased stability and the ability

[*] Prof. D. Cahen, Dr. H. Haick
Department of Materials and Interfaces,
Weizmann Institute of Science
Rehovot 76100 (Israel)
E-mail: david.cahen@weizmann.ac.il

Dr. M. Ambrico
CNR-IMIP and Dipartimento di Fisica
Universita' degli Studi di Bari
Sezione di Bari, Via Orabona 4, I-70126 Bari (Italy)

Dr. T. Ligonzo
Dipartimento di Fisica Universita' degli Studi di Bari and
Istituto Nazionale di Fisica della Materia
Sezione di Bari, Via Orabona 4, I-70126 Bari (Italy)

[**] We are grateful to the Israel Science Foundation, the Philip M. Klutznick Research Fund, and the Minerva foundation (Munich) for partial support. We thank our Weizmann Institute colleagues R. Arad-Yellin and A. Shanzer for the dC–X molecules, J. Ghabboun (Weizmann) and A. Kahn (Princeton University) for fruitful discussions, and G. Bruno (CNR-IMIP, Bari), V. Augelli and L. Schiavulli (Univ. Bari) for their support.